

Phonon structure in I - V characteristic of MgB_2 point contacts

I. K. Yanson,^{1,2,*} V. V. Fisun,¹ N. L. Bobrov,¹ Yu. G. Naidyuk,¹ W. N. Kang,³ Eun-Mi Choi,³ Hyun-Jung Kim,³ and Sung-Ik Lee³

¹*B. Verkin Institute for Low Temperature Physics and Engineering, National Academy of Sciences of Ukraine, 47 Lenin Avenue, 61103, Kharkiv, Ukraine*

²*Forschungszentrum Karlsruhe GmbH, Technik und Umwelt, Postfach 3640, D-76021, Karlsruhe, Germany*

³*National Creative Research Initiative Center for Superconductivity, Department of Physics, Pohang University of Science and Technology, Pohang 790-784, South Korea*

(Received 13 June 2002; revised manuscript received 13 August 2002; published 31 January 2003)

A search of the phonon structure at the above-gap energies was carried out for $d^2V/dI^2(V)$ spectra of MgB_2 point contacts with a normal metal. The two-band model is assumed not only for the gap structure in $dV/dI(V)$ characteristics, but also for phonons in $d^2V/dI^2(V)$ point-contact spectra, with up to the maximum lattice vibration energy. Since the current is carried mostly by charges of the three-dimensional (3D) band (π band), whereas the strong electron-phonon interaction occurs in 2D band (σ band), we observe the phonon peculiarities due to the “proximity” effect in k space, which depends on both the contact orientation with respect to the crystal axes and the variation of interband coupling through the elastic scattering.

DOI: 10.1103/PhysRevB.67.024517

PACS number(s): 74.25.Fy, 74.45.+c, 73.40.Jn

INTRODUCTION

The superconducting properties of the newly discovered s - p compound MgB_2 (Ref. 1) have been attracting the attention of the superconductive community recently. The relatively high $T_c \approx 39$ K, the absence of magnetic order, and strongly correlated charge carriers, on the one hand, and the strong links between grains for large enough critical currents and magnetic fields, on the other, make it very promising for a complete understanding of the superconducting mechanism and its successful applications at moderate temperatures.²

Unfortunately, the simplicity of this compound does not go too far for an immediate understanding of all details of its superconducting mechanism. From the theoretical point of view, this compound appears to be a rare example of several (at least two) disconnected bands of the Fermi surface (FS) with quite different dynamical properties.³⁻⁵ The theory predicts that one of those is two dimensional (2D), with a strong electron-phonon interaction (EPI), while the other is 3D with weak EPI and even larger density of states at the Fermi energy.⁴⁻⁷ The interband scattering between these two parts is weak,⁵ and they behave similar to an “intrinsic proximity effect.”⁸ The superconducting and normal parts are not separated spatially, as in the McMillan model^{9,10} of SN sandwiches, but are weakly connected in k space through the interband scattering. In connection with this behavior, one has to recall earlier works of two-band superconductivity.¹¹⁻¹³ But there is an important difference between the predictions of those old papers and what is observed in Ref. 8 and some other point-contact and tunneling works (see, for example, Refs. 14,15). Since the 2D and 3D parts of Fermi surface are very anisotropic, the tunneling and point-contact current depends strongly on the orientation with respect to the crystal axes, and for c orientation the contribution of the 3D band prevails.¹⁶ Superconducting energy gap values, corresponding to these two bands, differ very much [up to a factor of 3 (Refs. 16,17)], and turn to zero at the same critical temperature $\sim 38-40$ K. Moreover, if the

separate energy gaps converge to a single averaged gap, the critical temperature remains almost the same. Possible explanation of this behavior¹⁶ is that the charges of the 3D band play much greater role in the PC current, due to the higher Fermi velocity and larger plasma frequency. In analogy, the situation looks as if one measures superconducting energy gap only from the “normal” side of the McMillan sandwiches in coordinate space. T_c does not decrease noticeably with increasing elastic scattering, since 2D- and 3D-band orbitals, having different parity, are orthogonal in coordinate space, and the interband transitions are rare enough.¹⁸

Luckily, in MgB_2 no other bosonic excitation, except phonons, is anticipated.^{5,17,19} Thus, the only mechanism of the formation of Cooper pairs is EPI, although when a new superconductor with relatively high T_c is discovered, other mechanisms are always proposed.

In spite of great variety of spectroscopic measurements, which convincingly show the existence of two different superconducting energy gaps belonging to the above mentioned two parts of FS (see, for example, Refs. 14,20, and more recent papers^{8,15}), there are only a few reports of direct experimental proof for phonon structure in the point-contact characteristic²¹ or tunneling.²²

In this paper we present an attempt to identify the structure of MgB_2 point-contact (PC) spectra at energies up to the maximum phonon frequency. We show that the observed peculiarities are unequivocally caused by phonons, and their appearance correlates with the observed superconducting energy gap for a given point contact. In our opinion, this is due to the strong anisotropy of multiband electron and phonon spectra, and to the influence of the elastic scattering, which determines both the intraband and interband EPI coupling in this compound. The random deviation of the contact axis from the predominantly c direction plays a crucial role.

SPECIFICS OF EXPERIMENT

The samples are c -axis oriented films of MgB_2 , whose characteristics are described in Refs. 20,23. The contacts are

made by direct touch of MgB_2 with a sharpened normal metal electrode (Cu or Ag). The axis of the contact nominally coincides with the c axis of the film, and thus, determines the main direction of the current. The orientation selectivity in the point-contact spectroscopy is low (lower, than in plane tunnel junction, where it goes exponentially), and is within a solid angle of roughly a few tens of degrees. Moreover, since not every touch produces the desired appearance of the energy-gap I - V characteristic, we moved the electrodes relative to each other in order to penetrate through the accidentally damaged surface layer. This operation changes the contribution of the perpendicular ab direction and produces additional defects in the contact region and, thus, shortens further the small electron mean free path. In a few experiments we tried to make a contact with a broken sideface of the film, in order to increase the occurrence of the ab direction for the current.

Thus, our “input” characteristic is the shape of superconducting energy-gap structure, which is described elsewhere.^{20,21} The main goal is to investigate the first and second derivatives of the I - V characteristic at large biases, providing the contact survives the long-term measurements.

The attractive feature of PC spectroscopy is that the measured second derivative for the normal state turns out to be directly proportional to EPI function $\alpha^2(\omega)F(\omega)$ (Refs. 24,26)

$$\frac{d^2V}{dI^2} \propto \frac{d(\ln R)}{dV} = \frac{8ed}{3\hbar v_F} \alpha^2(\omega)F(\omega), \quad (1)$$

where α , roughly speaking, describes the strength of the electron interaction with one or another phonon branch for electron transport through the contact with diameter d and $F(\omega)$ stands for the phonon density of states. In PC spectra the EPI spectral function is modified by the transport factor, which increases strongly the back scattering processes.

However, in the superconducting state the above-gap singularity at phonon frequencies can be caused by several mechanisms.^{26,27} The features, which are strongly shifted along the voltage scale upon increasing the temperature and field, should be disregarded, as due to the nonequilibrium superconducting phenomena.^{26,27} Only those whose positions do not depend on T, H , except the small shifts of the order of superconducting energy gaps (2–7 meV), are considered.

The temperature is varied from 1.5 K up to $T \geq T_c$ with the magnetic field up to 4.5 T applied along the ab plane. At low temperatures this field is not enough to destroy superconductivity. In order to observe the inelastic point-contact spectrum in the normal state, we raise both the temperature and the field.

The magnetic field does not influence the inelastic PC spectrum (1), because of the short mean free path compared to Larmor radius. But it can strongly suppress superconductivity in the weakly superconducting 3D band, and destroy the exchange of the Cooper pairs from the strongly superconducting 2D band. Since the current flows mostly from the 3D band, the phonon structure appears indirectly, its intensity being strongly influenced by the field. Only small admixture

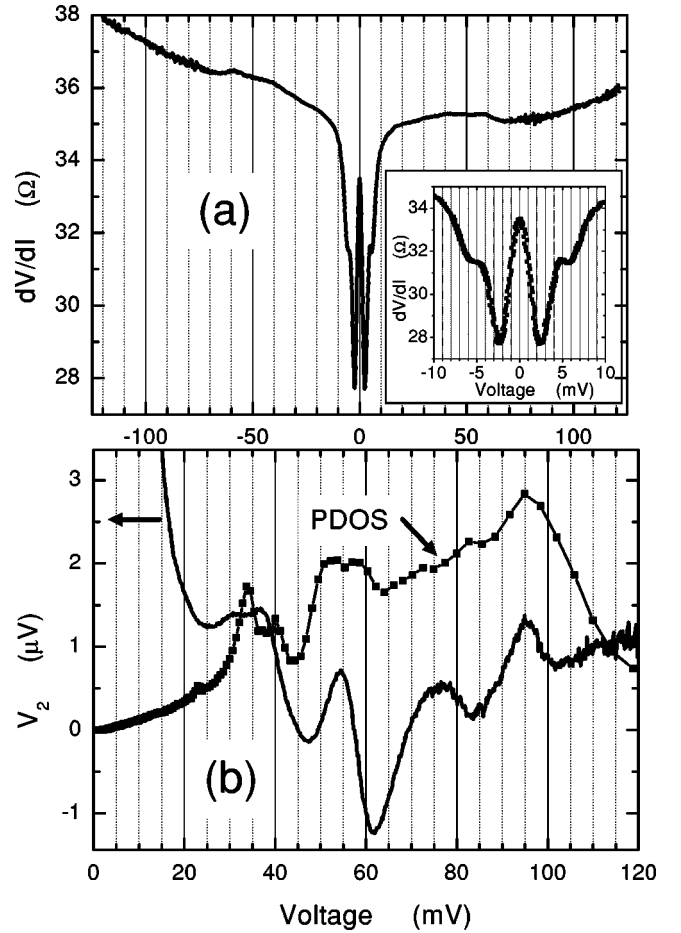


FIG. 1. (a) Differential resistance $R = dV/dI(V)$ for MgB_2 -Ag point contact. $T = 4.2$ K, $H = 0$, $R_0 = 35 \Omega$. In the inset, the structure at bias $\leq |10|$ mV is shown with two superconducting gaps corresponding to two different parts of the Fermi surface. The junction is made with the broken sideface of the film. (b) The point-contact spectrum averaged between plus and minus V -polarity for the same contact, as in panel (a). It is compared to the experimental phonon density of states of MgB_2 taken from Ref. 28. V_2 is the second harmonic voltage with modulation voltage $V_1 = 2.52$ mV. $d(\ln R)/dV = 2\sqrt{2}V_2/V_1^2$. The linear background is subtracted from the raw data. The ordinate axis for PDOS is given in arbitrary units.

of the direct 2D band contributes to EPI, due to random inclusion of the ab direction in the current.

RESULTS AND DISCUSSION

In Fig. 1(a) the $dV/dI(V)$ and $V_2(eV) \propto d^2V/dI^2(eV)$ characteristics are shown in the superconducting state at zero field. In the energy-gap region the two gaps are clearly seen with $\Delta_1 = 2.4$ and $\Delta_2 = 5.7$ meV. Further on, we simply denote by Δ the position of dV/dI minimum. For many junctions we determine the superconducting energy gap by the BTK-fitting procedure.²⁰ For PC with a not too large Γ parameter, introduced by Dynes, this value does not differ too much from the true energy gap. The first derivative at above-gap energies is slightly asymmetric and nearly parabolic, which leads to an approximately linear background in

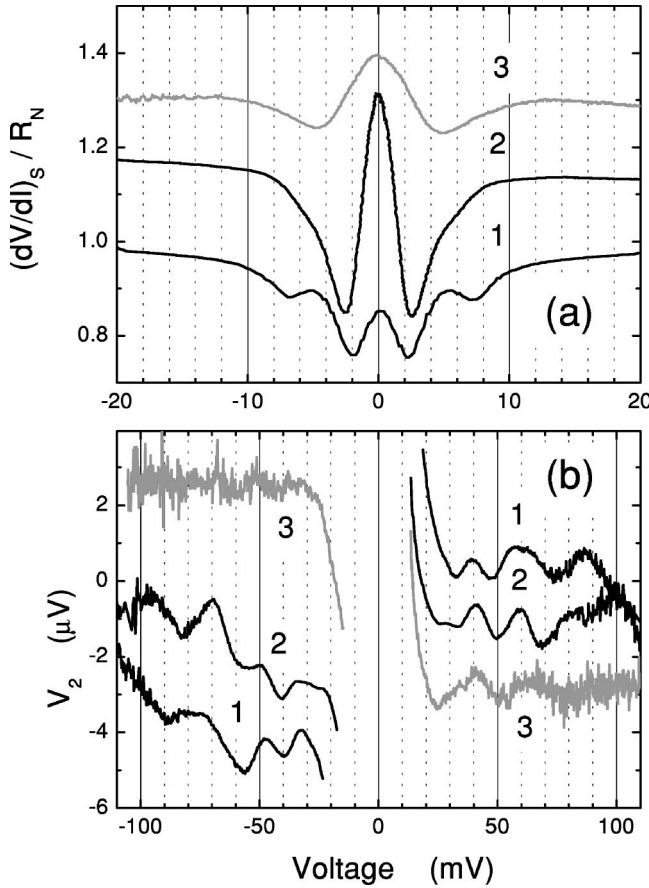


FIG. 2. (a) Differential resistance normalized to the normal state (taken as a resistance at $V \approx 30$ mV) for three different contacts with $R_0 = 45, 43,$ and 111Ω (curves 1–3, respectively). Main gap dV/dI minima are at about 2.1, 2.6, and 4.86 mV, correspondingly. The larger gap for curve 1 equals 7.0 meV. Curves 2,3 are shifted vertically for clarity. (b) Raw data of the second harmonic signal V_2 with modulation voltages $V_1 = 3.31, 2.78,$ and 2.5 mV, respectively. The numbers of curves are the same as in (a). $T = 4.2$ K, $H = 0$. Curves 1,2 are shifted vertically for clarity. Their center of symmetry has (0,0) coordinates.

$d^2V/dI^2(V)$. This background is subtracted from the raw $V_2(V)$ dependence. The latter curve displays an antisymmetric structure, whose amplitude is about a fraction of percent in differential resistance. In panel (b), this structure is compared with the phonon density of states (PDOS).²⁸ Good correspondence is seen between the positions of PDOS peaks and maxima in $d^2V/dI^2(V)$.

The reproducibility of this kind of PC spectra for different contacts can be seen in Figs. 2(a), 2(b), where the raw data for three different junctions are shown. Here, the contact resistance varies from 43 to 111 Ω with gap minima at $\Delta = 2.1, 2.6,$ and 4.86 meV, respectively. All the second derivative spectra (b) correlate with PDOS. The slight variation is probably due to the anisotropy and different scattering rates in the contacts. Compared with the theoretical EPI function for isotropic one-band model (see, for example, Refs. 6,7,19), the peak at $eV = 60\text{--}70$ meV of E_{2g} boron mode is not too much higher in intensity, in accord with our earlier observation.²¹ In contrast, for the two-band model, owing to

the point-contact current, we obtain an information mostly from 3D band. In this case, the theory predicts, that the EPI spectral function has the E_{2g} -peak intensity of the same order of magnitude as the other peaks of phonon density of states (see Fig. 1 in Ref. 29).

According to our classifications of the energy gap structure,²⁰ it is due to the random orientation of the contact axis and scattering of charge carriers between two band of Fermi surface, having gaps Δ_1 and Δ_2 mixed. With an increase of interband scattering the magnitude of Δ_1 (Δ_2) moves to the higher (lower) value, respectively. For dirty contacts, where the admixture of the 2D band is essential, only one maximum is seen with a broad distribution around ≈ 3.5 meV,²⁰ while T_c remains almost the same. In this case l is smaller than d (where l and d are the electron mean free path and the size of the contact, respectively), and the inelastic backscattering contribution to the phonon structure, proportional to l/d ,²⁵ is small. Therefore, in the superconducting state, the observed phonon structure presents mainly the elastic contribution to the excess current.²⁶ The elastic term is proportional to the energy dependent part of the excess current $I_{exc}(eV)$, similar to the phonon structure in the quasi-particle DOS for tunneling spectroscopy.^{26,27}

$$\frac{dI_{exc}}{dV}(eV) = \frac{1}{R_0} \left| \frac{\Delta_{in}(eV)}{eV + \sqrt{(eV)^2 - \Delta_{in}^2(eV)}} \right|^2, \quad (2)$$

where $\Delta_{in}(eV)$ is the gap parameter in the 3D band, induced by the 2D-band EPI. As seen in Fig. 2, if the Δ value increases [panel (a), curves 1–3], then the intensity of the phonon structure in the units of $d(\ln R)/dV = 2\sqrt{2}V_2/V_1^2$ increases too [panel (b)]. That is because the modulation voltage V_1 decreases, whereas the amplitudes in $V_2(eV)$ units remain approximately the same. Note, that for curve 1 in Fig. 2(a) one has to take the lower gap Δ_1 , because the current is mainly determined by the 3D band, as mentioned above.

In Fig. 3, the normal state spectrum is displayed together with the differential resistances in the superconducting state, showing the energy gap structure. In spite of a 10 time increase of the temperature smearing (≈ 20 meV at 41 K instead of 2 meV at 4.2 K), the residual phonon structure is still visible in Fig. 3(b). The smeared phonon features are superimposed on the rising linear background. For curve 2, we see an increase in scattering at ≈ 35 meV, where the acoustic phonon peak occurs, and the saturation at ≈ 100 meV, where the phonon spectrum ends. In the normal state, only those nonlinearities remain, which are due to the inelastic processes.²⁴ We stress that judging from the superconducting gap value [≈ 3.69 meV for curve 2 in panel (a)] the essential contribution is expected from the $\Delta_2(E)$ of 2D band. This spectrum should contrast with curve 6 in Fig. 4 (see below), where the contribution from the 2D band is small, due to lower value of Δ . Thus, the back scattering processes from the 3D band are mostly essential here. The shape of spectrum 1 in Fig. 3(b) presents the behavior intermediate between these two extremes, although its energy gap is approximately equal to curve 6 in Fig. 4. In addition to the

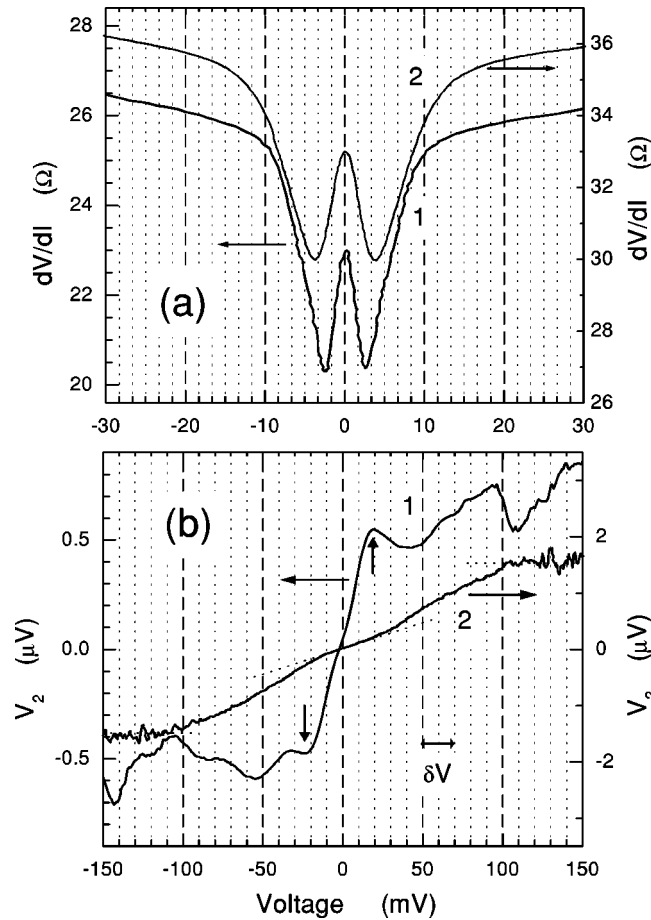


FIG. 3. (a) Differential resistances for $\text{MgB}_2\text{-Cu}$ point contacts, whose normal state spectra are presented in panel (b). $\Delta^{(1)} = 2.55$ meV, $\Delta^{(2)} = 3.69$ meV. $T = 4.2$ K, $H = 0$. (b) Second harmonic signals in the normal state. $V_1 = 2.2$ mV, $T = 41$ K. For spectrum No. 1 the vertical arrows mark the low frequency bumps at about 20 meV. The dotted tangent straight lines point to the phonon features on curve No. 2. The horizontal bar with double arrows stands for thermal smearing, determining the spectral resolution δV .

well seen phonon spectral features in the range 30–100 meV, it possesses a low energy bump at about 20 meV.

Note, that the modulation voltages for spectra 1,2 in Figs. 3(b) and 4 are the same. That means that they have the same second derivative scales, and the intensity of the second derivative is greater for curve 2 in Fig. 3(b), than those of curve 1 in Fig. 3(b) and curve 6 in Fig. 4.

The increasing second derivative of the I - V characteristic in the normal state is due to excess generation of nonequilibrium phonons at the contact. The PC spectra with phonon features in the normal state at $T \geq T_c$, similar to those shown in Fig. 3(b), usually exhibit the nonequilibrium phenomena in the superconducting state. These phenomena are mostly due to destruction of superconductivity in the vicinity of the contact, and lead to depression of the excess current.²⁶ It has already been noted that the positions of these nonlinearities are strongly influenced by the field and temperature, and should therefore be disregarded.

As to the spectacular electron-phonon spectrum, pre-

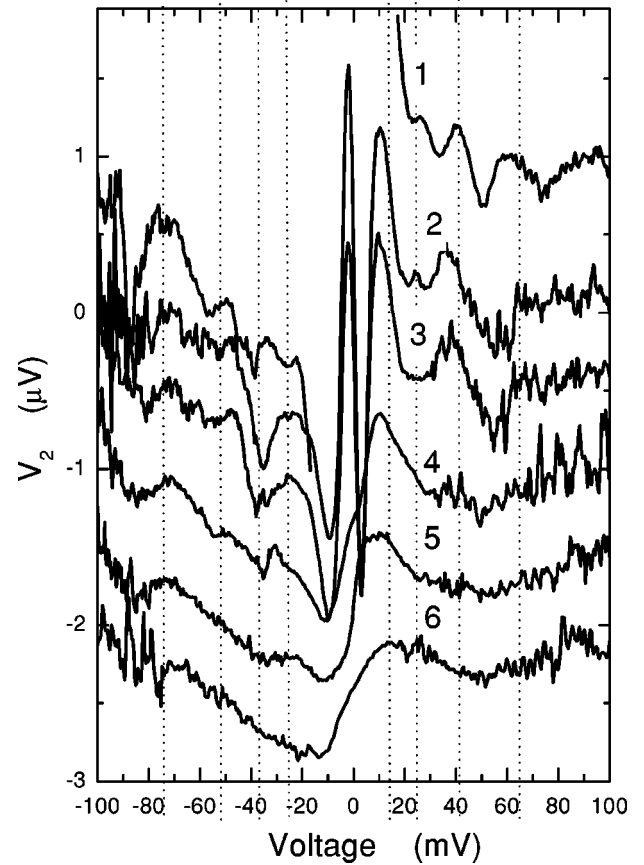


FIG. 4. Second harmonic dependences on field and temperature. The temperature and magnetic field are equal to 4.2 K, 0 T; 4.2 K, 4 T; 10 K, 4 T; 20 K, 4 T; 30 K, 4 T; 40 K, 0 T, for curves 1–6, respectively. The modulation voltage V_1 is 2.2 mV. $\Delta = 2.7$ meV. The vertical dotted lines mark the phonon singularity on the voltage axis. Curves are shifted vertically for clarity, their center of symmetry corresponding to (0,0) coordinates.

sented in our preliminary report (see Figs. 3, 4 in Ref. 21), it is presumably a rare example of a direct contribution from the inelastic spectrum Eq. (1) of the 3D band and should be compared with strongly broadened spectra in Fig. 3(b). The magnetic field of 4 T suppresses almost completely the induced phonon features Eq. (3) from the 2D band. Thus, the proposed tentative consideration would bring our previous observations in line with to what is consistently described here.

The phonon spectra of a contact with a small value of energy gaps are characterized by the presence of low frequency phonon peaks. The small peak at energy of about 25 meV (Fig. 4, curves 1,2) is visible, where a tiny knee exists on the PDOS (Ref. 28) [see PDOS in Fig. 1(b)]. In the normal state (at $T \geq T_c$), these low frequency peaks transform into the S-shape structure in $d^2V/dI^2(V)$ spectra (curve 6), corresponding to the wide minimum of $dV/dI(V)$ near zero bias. This low frequency structure is hardly due to the remnants of superconducting quasigap at $T > T_c$, since it is absent in junction No. 2, whose characteristic is shown in Fig. 3. Rather, it could be thought of as strong interaction in the 3D band with very low-frequency excitations, whose origin

is not clear yet. On increasing the temperature, the low frequency peak broadens further as common spectral features do in the normal state.

Since most of the current through the point contact is carried by the 3D band with weak EPI, the phonon singularity in the superconducting state is induced mainly by interband scattering from the 2D band with strong EPI. The degree of this induction depends on the interband coupling. As was noted above, in the clean limit the interband coupling in MgB_2 is low.⁵ That was the reason for applying the McMillan-proximity-effect model in order to fit the gap structure in $dI/dV(V)$ characteristic in Ref. 8. This model leads to the small-intensity phonon structure. The elastic scattering, which is certainly high in thin film and may be even stronger by point contact fabrication process, enhances the interband, as well as the intraband coupling. Following Arnold,³⁰ and assuming the extension of the proximity effect theory in coordinate space to the two-band model (i.e., “proximity” effect in k space), we use the corresponding expression for the interband coupling, induced by elastic scattering in SN sandwiches. In our case, by analogy, the elastic scattering leads to the expression

$$\Delta_1(E) = \frac{Z_1^p \Delta_1^p + i(\hbar/2\tau) \Delta_2(E) N_2(E)}{Z_1^p(E) + i(\hbar/2\tau) N_2(E)}, \quad (3)$$

which, similar to the McMillan expression for $\hbar/2\tau = \Gamma_N$ (not shown), derives to $\Delta_1(E) \approx \Delta_2(E)$, in other words, to the large induced phonon structure in the 3D band. Here Z_1^p is the renormalization function in the 3D band, $N_2(E)$ is the electron DOS in the 2D band, τ is the elastic scattering time, and Γ_N is the interband scattering rate in the McMillan model. Thus, as the interband scattering increases, the intensity of phonon singularity moves to the higher energy, characteristic of the 2D band. This “internal proximity effect” explains also the small variation in the position (of the order of superconducting energy gap) of phonon peaks with various elastic scattering rates produced by contact fabrication.

The influence of magnetic field on the point-contact spectra is shown in Fig. 4 (compare curves 1 and 2). It is evident that the field can smear out the intensity of high energy peaks, which are induced in the 3D band by EPI of the 2D band. The disappearance of phonon peaks at rising field and temperature proves that they do not belong to the inelastic back scattering processes, which should have the same intensity both in the superconducting and in normal states. It seems more plausible that the high energy phonon peaks are due to the elastic contribution in the excess current (2) induced by EPI from the 2D band, as was already stated above.

Unfortunately, we cannot estimate the strength of EPI by inelastic PC spectroscopy,²⁴ since we are not able to destroy

the superconductivity completely by magnetic field at low enough temperature. The latter is necessary to get good resolution. For thin films this experiment will hardly promise encouraging results, since the elastic mean free path is strongly reduced, and the intensity of inelastic backscattering processes is therefore diminished by the factor l/d . Note, that for the superconducting self-energy effects the short elastic mean free path does not suppress essentially the phonon structure.²⁶ On the contrary, for the two-band model elastic scattering even enhances the phonon structure due to the “intrinsic proximity effect” described above.

CONCLUSIONS

We summarize our observation as follows. The reproducible phonon peaks are seen in the superconducting state on $d^2V/dI^2(V)$, and disappear in the normal state, which proves that they are due to the energy dependence of superconducting order parameter. The superconductivity is presumably due to the 2D-band EPI, which induces the $\Delta(E)$ structure in the 3D band. At a small value of the superconducting gap the phonon structure is weak, and its intensity begins to increase with growing Δ . The robustness against the magnetic field also grows notably with increasing Δ .

In the normal state the intensity of the inelastic spectrum also correlates with the value of the superconducting gap. The tendency is observed that the high energy phonons become more prominent for a larger gap. For a smaller gap, the low-frequency bump appears in the spectra. It might be due to EPI with some unknown low-frequency excitation,³¹ but further work is needed to be sure that it is not caused by phonon peaks of the normal-metal counter electrode (Cu, Ag).

The final goal of PC spectroscopy is to use sufficiently clean material at low temperatures in high enough magnetic field, in order to suppress superconductivity and estimate quantitatively the strength of EPI. The PC experiment, including single crystal technology development, should go in parallel with theoretical calculation, taking into account the specific transport form factor.²⁴

ACKNOWLEDGMENTS

The work in Ukraine was supported by the State Foundation of Fundamental Research, Grant No. F7/528-2001. I.K.Y. is grateful to Forschungszentrum Karlsruhe for hospitality, and thanks Dr. Renker for MgB_2 phonon spectrum from Ref. 28. The work at Postech was supported by the Ministry of Science and Technology of Korea through the Creative Research Initiative Program.

*Email address: yanson@ilt.kharkov.ua

¹J. Nagamatsu, N. Nakagawa, T. Muranaka, Y. Zenitani, and J. Akimitsu, *Nature (London)* **410**, 63 (2001).

²D. M. Buzea and T. Yamashita, *Semicond. Sci. Technol.* **14**, R115 (2001).

³S. V. Shulga, S.-L. Drechsler, H. Eschrig, H. Rosner, and W. E.

Pickett, *cond-mat/0103154* (unpublished).

⁴J. Kortus, I. I. Mazin, K. D. Belashchenko, V. P. Antropov, and L. L. Boyer, *Phys. Rev. Lett.* **86**, 4656 (2001).

⁵A. Y. Liu, I. I. Mazin, and J. Kortus, *Phys. Rev. Lett.* **87**, 087005 (2001).

⁶Y. Kong, O. V. Dolgov, O. Jepsen, and O. K. Andersen, *Phys.*

- Rev. B **64**, 020501(R) (2001).
- ⁷T. Yildirim, O. Gülseren, J. W. Lynn, C. M. Brown, T. J. Udovic, Q. Huang, N. Rogado, K. A. Regan, M. A. Hayward, J. S. Slusky, T. He, M. K. Haas, P. Khalifah, K. Inumaru, and R. J. Cava, Phys. Rev. Lett. **87**, 037001 (2001).
 - ⁸H. Schmidt, J. F. Zasadzinski, K. E. Gray, and D. G. Hinks, Phys. Rev. Lett. **88**, 127002 (2002).
 - ⁹W. L. McMillan, Phys. Rev. **175**, 537 (1968).
 - ¹⁰E. L. Wolf, *Principles of Electron Tunneling Spectroscopy* (Oxford University Press, Oxford, 1985).
 - ¹¹H. Suhl, B. T. Matthias, and L. R. Walker, Phys. Rev. Lett. **3**, 552 (1959).
 - ¹²C. C. Sung and V. K. Wong, J. Phys. Chem. Solids **28**, 1933 (1967).
 - ¹³V. P. Galaiko, Fiz. Nizk. Temp. **13**, 1102 (1987) [Sov. J. Low Temp. Phys. **13**, 627 (1987)].
 - ¹⁴F. Laube, G. Goll, J. Hagel, H. v. Löhneysen, D. Ernst, and T. Wolf, Europhys. Lett. **56**, 296 (2001).
 - ¹⁵M. Iavarone, G. Karapetrov, A. E. Koshelev, W. K. Kwok, G. W. Crabtree, D. G. Hinks, W. N. Kang, Eun-Mi Choi, Hyun Jung Kim, Hyeong-Jin Kim, and S. I. Lee, Phys. Rev. Lett. **89**, 187002 (2002).
 - ¹⁶A. Brinkman, A. A. Golubov, H. Rogalla, O. V. Dolgov, J. Kortus, Y. Kong, O. Jepsen, and O. K. Andersen, Phys. Rev. B **65**, 180517 (2002).
 - ¹⁷Hyoungh Joon Choi, David Roundy, Hong Sun, Marvin L. Cohen, and Steven G. Louie, Nature (London) **418**, 758 (2002).
 - ¹⁸I. I. Mazin, O. K. Andersen, O. Jepsen, O. V. Dolgov, J. Kortus, A. A. Golubov, A. B. Kuz'menko, and D. van der Marel, Phys. Rev. Lett. **89**, 107002 (2002).
 - ¹⁹K.-P. Bohnen, R. Heid, and B. Renker, Phys. Rev. Lett. **86**, 5771 (2001).
 - ²⁰Yu. G. Naidyuk, I. K. Yanson, L. V. Tyutrina, N. L. Bobrov, P. N. Chubov, W. N. Kang, Hyeong-Jin Kim, Eun-Mi Choi, and Sung-Ik Lee, JETP Lett. **75**, 238 (2002).
 - ²¹N. L. Bobrov, P. N. Chubov, Yu. G. Naidyuk, L. V. Tyutrina, I. K. Yanson, W. N. Kang, Hyeong-Jin Kim, Eun-Mi Choi, and Sung-Ik Lee, cond-mat/0110006, in *Quantum Mesoscopic Phenomena and Mesoscopic Devices in Microelectronics*, edited by J. F. Annett and S. Kruchinin (Kluwer Academic, 2002), p. 225.
 - ²²A. I. D'yachenko, V. Yu. Tarenkov, A. V. Abal'oshev, and S. J. Lewandowski, cond-mat/0201200 (unpublished).
 - ²³W. N. Kang, Hyeong-Jin Kim, Eun-Mi Choi, C. U. Jung, and Sung-Ik Lee, Science **292**, 1521 (2001); Hyeong-Jin Kim, W. N. Kang, Eun-Mi Choi, Mun-Seog Kim, Kijoon H. P. Kim, and Sung-Ik Lee, Phys. Rev. Lett. **87**, 087002 (2001).
 - ²⁴I. O. Kulik, A. N. Omelyanchouk, and R. I. Shekhter, Sov. J. Low Temp. Phys. **3**, 740 (1977).
 - ²⁵I. O. Kulik and I. K. Yanson, Sov. J. Low Temp. Phys. **4**, 596 (1978).
 - ²⁶I. K. Yanson, in *Quantum Mesoscopic Phenomena and Mesoscopic Devices in Microelectronics*, edited by I. O. Kulik and R. Ellialtioglu (Kluwer Academic, Dordrecht, 2000), pp. 61–77.
 - ²⁷A. N. Omel'yanchuk, S. I. Beloborod'ko, and I. O. Kulik, Sov. J. Low Temp. Phys. **14**, 630 (1988).
 - ²⁸B. Renker, K. B. Bohnen, R. Heid, D. Ernst, H. Schober, M. Koza, P. Adelman, P. Schweiss, and T. Wolf, Phys. Rev. Lett. **88**, 067001 (2002).
 - ²⁹A. A. Golubov, J. Kortus, O. V. Dolgov, O. Jepsen, Y. Kong, O. K. Andersen, B. Gibson, K. Ahn, and R. K. Kremer, J. Phys.: Condens. Matter **14**, 1353 (2002).
 - ³⁰G. B. Arnold, Phys. Rev. B **23**, 1171 (1981).
 - ³¹D. Lampakis, A. Tatsi, E. Liarokapis, G. Varelogiannis, P. M. Oppeneer, M. Pissas, and T. Nishizaki, cond-mat/0105447 (unpublished).